Second, the present work does not take account of effects arising from the nonlocal character of the pseudopotential. In the (nonlocal) Heine-Abarenkov approximation [V. Heine and I. Abarenkov, Phil. Mag. 9, 451 (1964)], the Si and Ge pseudopotentials differ principally in their scattering of d waves [A. O. E. Animalu and V. Heine, Phil. Mag. 12, 1249 (1965)], not s waves as in the present model. This presumably reflects the fact that the Ge ion has a filled d shell, which the Si ion lacks. However, as in the present model, the Heine-Abarenkov pseudopotential is the same for Si and Ge ions outside a certain core radius.

Since it is not obvious how these various effects would modify the observed broadenings in Si_xGe_{1-x}, our numerical results should be considered in the spirit of a pilot calculation. It should be emphasized, however, that the present formalism may readily be generalized to more realistic nonlocal pseudopotential models from which band broadenings could be more accurately calculated.

We are grateful to M. Cardona, J. C. Phillips, and B. O. Seraphin for enlightening discussions of these questions.

*Supported in part by Grant No. GP-8019 of the National Science Foundation and the Advanced Research Projects Agency.

†Present address: Laboratory of Atomic and Solid State Physics, Clark Hall, Cornell University, Ithaca, N. Y. 14850.

[1]P. Soven, Phys. Rev. 156, 809 (1967).
[2]D. W. Taylor, Phys. Rev. 156, 1017 (1967).
[3]Y. Onodera and Y. Toyozawa, J. Phys. Soc. Japan 24, 341 (1968).
[4]B. Velický, S. Kirkpatrick, and H. Ehrenreich, Phys. Rev. 175, 747 (1968).
[5]P. Soven, Phys. Rev. 178, 1136 (1969).
[6]S. Kirkpatrick, B. Velický, and H. Ehrenreich, Phys. Rev. (to be published).
[7]A detailed discussion of the numerical methods and approximations used is to be found in D. Stroud, Ph. D. dissertation, Harvard University, 1969 (unpublished).
[8]F. Herman, Phys. Rev. 95, 847 (1954).
[9]J. Tauc and H. Abrahám, J. Phys. Chem. Solids 20, 190 (1961).
[10]F. Bassani and D. Brust, Phys. Rev. 131, 1524 (1963).
[11]See, for example, P. Nozières, *Theory of Interacting Fermi Systems* (Benjamin, New York, 1963), pp. 345–51.
[12]B. J. Austin, V. Heine, and L. J. Sham, Phys. Rev. 127, 276 (1962).
[13]P. Lloyd, Proc. Phys. Soc. (London) 90, 207 (1967).
[14]Yu. A. Izyumov, Advan. Phys. 14, 569 (1965).
[15]D. Brust, Phys. Rev. 134, A1337 (1964).
[16]E. Schmidt, Phys. Status Solidi 27, 57 (1968).
[17]I. M. Lifshitz, Usp. Fiz. Nauk. USSR 83, 617 (1964) [Soviet Phys. Usp. 7, 549 (1965)].
[18]E. R. Johnson and S. M. Christian, Phys. Rev. 95, 560 (1954).
[19]R. Braunstein, A. R. Moore, and F. Herman, Phys. Rev. 109, 695 (1958).
[20]B. Velický, Phys. Rev. (to be published).

PHYSICAL REVIEW B VOLUME 2, NUMBER 8 15 OCTOBER 1970

Anistropy of the Constant-Energy Surfaces in n-Type Bi_2Te_3 and Bi_2Se_3 from Galvanomagnetic Coefficients*

L. P. Caywood, Jr.,† and G. R. Miller
University of Utah, Salt Lake City, Utah 84112
(Received 17 November 1969)

Low-field galvanomagnetic coefficients have been measured on single crystals of Bi_2Te_3 and Bi_2Se_3 at 76 °K in fields to 9 kG. Using a six-valley ellipsoid model in the isotropic relaxation-time approximation, the mass parameters of the ellipsoids are calculated for both compounds. The discrepancy between previously reported galvanomagnetic data and de Haas–van Alphen data for Bi_2Te_3 can be minimized by recalculating the mass parameters from the galvanomagnetic data and by not assuming complete degeneracy. The experimental data on Bi_2Te_3 are in agreement with those reported earlier. There is also very good evidence of second-band effects at high electron concentrations ($> 10^{19}$ cm^{-3}), as has been previously suggested. The constant-energy surfaces undergo an apparent change in shape between low- and high-concentration samples. Data on Bi_2Se_3 indicate that the constant-energy surfaces are more spherical than in the case of Bi_2Te_3.

I. INTRODUCTION

Because of their possible application in efficient thermoelectric devices, the intermetallic compounds Bi_2Te_3 and Bi_2Se_3 and their alloys have received a great deal of attention in the last decade. An extensive literature is available and several review

articles and data sheets have emerged.[1-4] Investigations published within the past few years, however, have indicated certain discrepancies in the details of the conduction bands of these two compounds.

In the case of Bi_2Te_3, two problems have arisen. First, the details of the conduction bands are questioned because of discrepancies between recent de Haas–van Alphen (dHvA) measurements[5] and the earlier galvanomagnetic (GM) work of Drabble *et al.*[6] In the effective-mass determinations of Ref. 5, the orientation of the major axes of the constant-energy ellipsoids is such that the ellipsoidal energy surfaces are compressed in a direction parallel to the binary axis. The GM data of Ref. 6, however, indicates that the ellipsoids are compressed in a direction almost parallel to the bisectrix axis. Second, the existence of another, higher-lying conduction band in Bi_2Te_3 has been postulated from Hall and dHvA studies.[5] Such a band would help to explain the seemingly nonparabolic nature of the single conduction band proposed by Goldsmid[1] and others.[7,8]

Little work has been performed on the conduction-band structure of Bi_2Se_3, possibly because the marked nonstoichiometry of the compound gives rise to a highly degenerate n-type material and renders the usual techniques for effective-mass parameter measurement very difficult. Hashimoto[9] has calculated effective-mass parameters for Bi_2Se_3 using GM measurements. He reports carrier concentrations which vary from 2.25×10^{19} to 2.15×10^{17} cm^{-3} for samples of the same composition. This suggests a need for further work on Bi_2Se_3.

It is the purpose of this study to resolve these discrepancies and to provide reasonable data on which to base a determination of the existence of a second conduction band in Bi_2Te_3. The authors chose the method of GM coefficients both because of its relative experimental simplicity and because the previous studies of Drabble *et al.*[6] on Bi_2Te_3 and Hashimoto[9] on Bi_2Se_3 were carried out in this general manner.

II. MANY-VALLEY MODEL AND TRANSPORT EQUATIONS

Both Bi_2Te_3 and Bi_2Se_3 have a trigonal unit cell, with five atoms per cell, and possess point group symmetry $R\bar{3}m$ (see Fig. 1). The major symmetry elements are (a) an inversion center, (b) a threefold axis, (c) three reflection planes parallel to the threefold axis, and (d) three twofold axes lying half-way between the reflection planes. The first Brillouin zone[10] is shown in Fig. 2 and corresponding crystallographic data are listed in Table I.[5] For the subsequent analysis, we will use the Cartesian coordinate system defined by Mallinson *et al.*[5] and Hashimoto[9] since this is the conventional notation used in the bismuth literature. In this system, the $x(1)$ axis (binary direction) is along the twofold axis, the $y(2)$ axis (bisectrix) is in the reflection plane, and the $z(3)$ (trigonal) direction is parallel to the threefold rotation axis. Unfortunately, a second system in which the x and y axes are interchanged is used in much[6,11] of the Bi_2Te_3 literature.

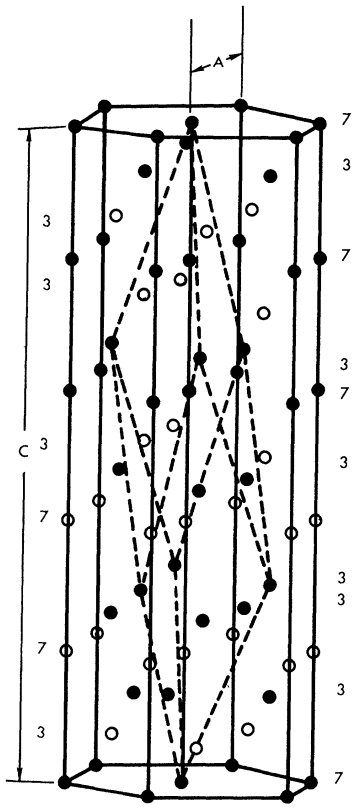

FIG. 1. Crystal structure of Bi_2Te_3. The dark circles represent tellurium atoms and the open circles represent bismuth atoms. Bi_2Se_3 crystallizes with the same structure. Numbers at the edge of the drawing indicate the number of atoms in each layer. The primative trigonal unit cell is indicated with dashed lines and contains two Bi atoms and three Te atoms. A hexagonal unit cell is shown with solid lines and contains 18 Bi atoms and 27 Te atoms. The C axis is 30.5 Å while the A axis is 4.38 Å.

In relating the effective-mass tensor to the measurable transport coefficients, we use the six-valley conduction-band model shown by several investigators to be adequate for Bi_2Te_3.[5,12-15] The six-valley model is by analogy assumed correct for Bi_2Se_3. Hashimoto[9] was able to show that a six-valley model holds; however, on the basis of data reported in this paper, his results were not accurate enough to make that judgment. The effective-mass ratios reported herein hold for a six- or three-valley model. The energy surfaces are assumed to be

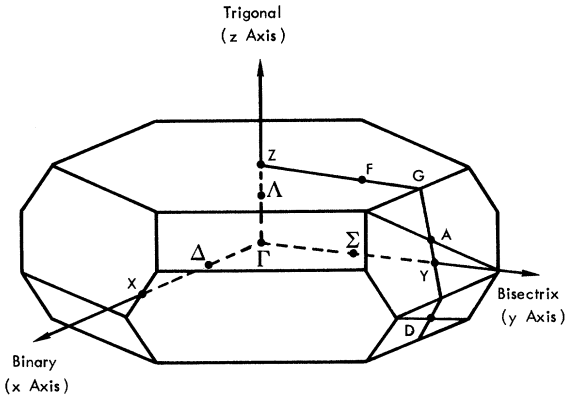

FIG. 2. Brillouin zone of Bi_2Te_3. The drawing is extended in the Γz direction for clarity.

ellipsoids centered on the reflection planes and removed from the zone boundaries. We write the expression for the constant-energy surfaces in the ith valley as

$$E = E_0 + (\hbar^2/2m_0)\,(\vec{k}^{(i)} - \vec{k}_0)\cdot \overleftrightarrow{\alpha} \cdot (\vec{k}^{(i)} - \vec{k}_0) \quad , \qquad (1)$$

where E_0 is the energy at the ellipsoid center $\vec{k}_0$, $\vec{k}^{(i)}$ is the electron wave vector, m_0 is the free-electron mass, and $\overleftrightarrow{\alpha}$ is the inverse-mass tensor. In this expression, the reference axes are the crystal axes. For the six-valley model, the nonzero terms in the effective-mass tensor are α_{11}, α_{22}, α_{33}, and α_{23}, where α_{23} is an indication of the amount of rotation of the ellipsoid about the crystal x axis. A positive rotation angle θ is defined by the right-hand rule about the positive x axis. Expressions for the resistivities, Hall resistivity, and magnetoresistivity as given by Keys[16] and Drabble[17] are derived from the phenomenological isothermal current-field relations

$$E_i = \rho_{ij}J_j + \rho_{ijk}J_jH_k + \rho_{ijkl}J_jH_kH_l + \cdots$$

using the classical Boltzmann equation in the relaxation-time approximation. The summation convention is used.

An isotropic relaxation time is assumed which is a scalar function of energy $\tau \propto E^{-\lambda}$ then

$$\rho_{11} = \frac{2}{\alpha_{22} I_0 3N(1+u)} \quad , \quad \rho_{33} = \rho_{11}\frac{1+u}{2v} \quad ,$$

$$\rho_{213} = \frac{I_1 4u}{I_0^2\, 3N(1+u)^2} \quad , \quad \rho_{321} = \rho_{213}(w+uv)\frac{1+u}{4uv} \quad ,$$

$$\rho_{1111} = \frac{I_2\alpha_{22}\,(w - 5uw + 3uv + u^2v)}{I_0^2\, 6N(1+u)^2}$$

$$= \frac{b\,(w - 5uw + 3uv + u^2v)\,(1+u)}{16Bu^2} \quad ,$$

$$\rho_{1122} = b\left[\left(\frac{(3w + uw + uv + 3u^2v)\,(1+u)}{16Bu^2}\right) - \left(\frac{2v}{a^2(1+u)}\right)\right] ,$$

$$\rho_{1133} = b\left(\frac{(1+u)^2}{4uB} - 1\right) , \quad \rho_{3333} = b\,\frac{(1+u)^3(v-w)}{8\,Buv^2} \quad , \qquad (2)$$

$$\rho_{3311} = b\left(\frac{(1+u)^3(w+uv)}{16\,Bu^3v} - \frac{1}{a^2}\right),$$

$$\rho_{1132} = \frac{b(u^2-1)\,(v-w)^{1/2}}{8\,Bu} \quad ,$$

$$\rho_{3211} = b\,\frac{(u+1)^2\,(uv-w)\,(v-w)^{1/2}}{16\,Bu^2v} \quad ,$$

$$\rho_{2323} = \tfrac{1}{2}b\left(\frac{-(u+1)^2}{4uB} + \frac{1}{a}\right),$$

$$u = \frac{\alpha_{11}}{\alpha_{22}} \quad , \quad v = \frac{\alpha_{33}}{\alpha_{22}} \quad , \quad w = \frac{\alpha_{22}\alpha_{33} - \alpha_{23}^2}{\alpha_{22}^2} \quad ,$$

$$b \equiv \frac{\rho_{213}^2}{\rho_{11}} \quad , \quad B \equiv \frac{I_1^2}{I_0 I_2} \quad , \quad a \equiv \frac{\rho_{213}}{\rho_{321}} \quad ,$$

TABLE I. Crystallographic data for Bi_2Te_3 (See Ref. 5).

Symbol	Magnitude	Magnitude (units of b)	Definition
$\vec{a}$	10.418 Å		Rhombohedral vector at 0 °K
α	24 °12′40″		Rhombohedral angle at 0 °K
$\vec{b}$	1.6731 Å^{-1}	1.000	Reciprocal lattice vector
β	61 °30′37″		Rhombohedral angle for reciprocal lattice
V	169.11 Å^3		Unit cell volume
ΓA	0.8366 Å^{-1}	0.5000	$\frac{1}{2}$ (100)
ΓD	0.8556 Å^{-1}	0.5114	$\frac{1}{2}$ (110)
ΓZ	0.3108 Å^{-1}	0.1858	$\frac{1}{2}$ (111)
θ_1	7 °6′50″		Angle between ΓA and ΓY
θ_2	14 °0′50″		Angle between ΓD and ΓY

$$I_n \equiv -\left(\frac{e}{m}\right)^n \frac{e^2}{3\pi^2 m}\left(\frac{2m}{\hbar^2}\right)^{3/2} \times \frac{1}{\Delta^{1/2}}\int_0^\infty \tau^{n+1} E^{3/2}\frac{\partial f_0}{\partial E}\, dE \ ,$$

$$\Delta \equiv |\alpha_{ij}| = \alpha_{11}(\alpha_{22}\alpha_{33} - \alpha_{23}^2) \ .$$

For a three-valley model $N=1$, and for a six-valley model $N=2$. The x and y axes have been interchanged from those used by Drabble[17] and the symmetry relations given by Smith *et al.*[18] have been used. Sign errors in the expressions for ρ_{1132} and ρ_{3211}[17] have been corrected.

Drabble *et al.*[6] express the conductivity components in terms of effective-mass elements defined relative to the principal axis of an ellipsoid. Mallinson *et al.*[5] express their results in terms of an inverse effective-mass tensor $\overleftrightarrow{\alpha}$ which is defined relative to the crystal axis such that

$$\overleftrightarrow{\alpha}_{\text{crystal}} = m_0 \overleftrightarrow{T}(\theta)\cdot\overleftrightarrow{m}^{-1}\overleftrightarrow{T}^{-1}\cdot(\theta) \ , \qquad (3)$$

where

$$\overleftrightarrow{T}(\theta) = \begin{pmatrix} 1 & 0 & 0 \\ 0 & \cos\theta & \sin\theta \\ 0 & -\sin\theta & \cos\theta \end{pmatrix} .$$

The angle θ is defined as a rotation in the positive sense about the x axis which will carry the y axis of the ellipsoidal valley into the y axis of the crystal.

The mass ratios and the tilt angle of the principal axes can be calculated from Eq. (3),

$$\frac{m_1}{m_3} = \frac{w}{u(vs^2 + 2cs\,\alpha_{23}/\alpha_{22} + c^2)} \ ,$$

$$\frac{m_3}{m_2} = \frac{s^2 v + 2cs\,\alpha_{23}/\alpha_{22} + c^2}{s^2 - 2cs\,\alpha_{23}/\alpha_{22} + c^2 v} \ , \qquad (4)$$

$$\tan 2\theta = 2\alpha_{23}/(\alpha_{33} - \alpha_{22}) \ ,$$

where

$$s = \sin\theta \text{ and } c = \cos\theta \ .$$

The most serious assumption made in applying the transport equations to an anisotropic solid such as Bi_2Te_3 may be that of assuming a single isotropic relaxation time τ.

Several authors[19-25] have discussed the validity of using an isotropic relaxation time and its relationship to the effective-mass tensor. There are two treatments, one due to Korenblit,[24] and to Efimova, Korenblit, Novikov, and Ostroumov,[25] and the other due to Mackey and Sybert,[26] which we could use with an anisotropic relaxation time to evaluate our data.

The first requires very accurate values of the cross-field magnetoresistivity coefficients, e.g., ρ_{1132}. These coefficients are very dependent upon proper probe alignment. At 9 kG, the fractional change in the zero-field resistivity ($\Delta\rho/\rho$) may be as small as 0.0086% for this coefficient. We were not able to obtain those coefficients to the accuracy required for use with the Korenblit treatment.

The treatment of Mackey and Sybert[26] was based upon a highly degenerate Fermi-Dirac distribution. This distribution was found not to hold for Bi_2Te_3 or Bi_2Se_3 at 76 °K. We, therefore, were forced to treat our data in the approximation where τ was an isotropic function of energy.

In order to assess the qualitative merit of this approximation, we note that Herring[20] has found that in order for $\overleftrightarrow{\tau}(E)$ to be expressed as a scalar, the constant-energy surfaces must be very nearly isotropic if scattering is by ionized impurities. If the scattering mechanism is by intravalley acoustic-mode scattering, the energy surfaces must be very anisotropic in order to treat $\overleftrightarrow{\tau}(E)$ as a scalar. One, or a mixture of these two mechanisms, is probably responsible for scattering in Bi_2Se_3 and Bi_2Te_3.

As mentioned earlier, the existence of a six-valley ellipsoidal model for Bi_2Te_3 is well accepted. In particular, the dHvA and high-field Hall measurements by Mallinson *et al.*[5] have verified the existence of six valleys. The dHvA measurements are used to measure the extremal cross sections of the ellipsoids. This model has not yet been verified for Bi_2Se_3.

III. EXPERIMENTAL

A. Procedure

Single-crystal samples of Bi_2Te_3 and Bi_2Se_3 were grown using the Bridgman technique with ASARCO 99.999%+ Bi, Te, and Se. Most samples were cut using a wire saw with a 600-mesh silicon carbide slurry. The best crack-free samples were most easily obtained with an acid saw. For cutting Bi_2Te_3 samples, a solution of one part HCl to one part HNO_3 was used. For Bi_2Se_3, a one part HCl, three parts HNO_3 solution was found satisfactory. Sample orientations were determined using the backreflection Laue technique.[27]

After cutting, a technique developed by Sagar and Faust[28] was used to etch the crystals in a dilute solution of bromine in methanol. The crystals were then examined microscopically for small cracks which had been clearly revealed by the etching process. Crack-free samples were obtained which measured about 10× 2×1 mm. The sample length-to-width ratio was always greater

than 4:1.

Resistivity probes (electrical leads) were constructed with rigidly mounted tungsten needles having 1-mil-diam tungsten-carbide tips. The Hall probe was spring-mounted. These probes provided Ohmic contacts and were small enough to minimize electric field distortions.

All measurements were made at 76 °K. Temperatures were determined by a copper-constantan thermocouple calibrated with a 200-Ω platinum resistance thermometer. Magnetic fields to 10 kG were provided by a 7-in. Magnion L – 25B magnet. Potential measurements were obtained with a Biddle Gray model No. 605001-1 six-dial potentiometer and nanovolt null detector. This system was capable of voltage reproducibility to 0.01 μV.

B. Results

Checks were made of the Ohmic nature of the sample-probe contacts by reading magnetovoltage as a function of current. In order to verify the low-field approximation, Hall voltage was measured as a function of magnetic field and magnetovoltage was measured as a function of field. Results are shown in Figs. 3–5.

The carrier concentrations have been calculated from

$$n=\frac{rG_{213}}{e\rho_{213}}\,,\quad \frac{r}{ne}=\frac{I_1}{I_0^2\,3N}\,,\quad \text{and } G_{213}=\frac{4u}{(1+u)^2}\,. \tag{5}$$

In the high-field limit, $w\tau \gg 1$, r and G_{213} are equal to one. In the low-field case, this is not true. G_{213} can then be calculated from the shape parameters,

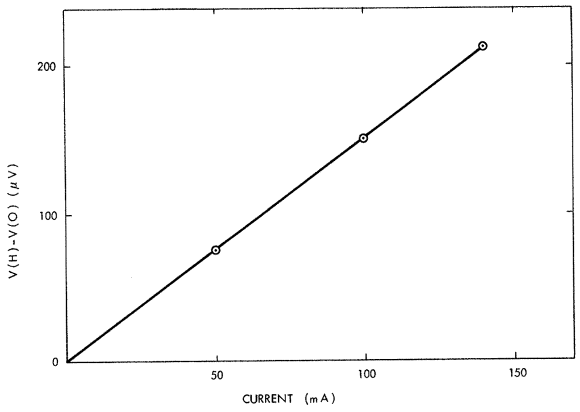

FIG. 3. Dependence of magnetovoltage on current for Bi_2Te_3 sample R2 at 5 kG and 76 °K.

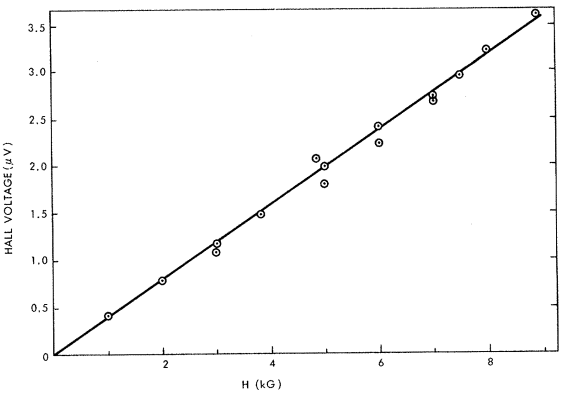

FIG. 4. Dependence of Hall voltage on magnetic field. Bi_2Se_3 sample R12A with a current of 10 mA at 76 °K.

while knowledge of the scattering mechanism and distribution function is required to solve for r; i.e., $r=1$ for degenerate acoustic-mode scattering and $r=\frac{3}{8}\pi$ for nondegenerate acoustic-mode scattering. Unless otherwise stated, carrier concentrations are reported for r and G_{213} equal one because, while G_{213} can be calculated, r cannot be calculated until the scattering mechanism is known. Carrier concentrations reported from low-field data must be corrected to obtain the actual concentration. The ρ_{213} Hall coefficient is measured with the current in the x-y plane parallel to the long axis of the sample. The magnetic field is along the z axis.

Galvanomagnetic coefficients measured on seven single crystals of Bi_2Se_3 are given in Table II. Data on samples of Bi_2Se_3 doped with 1-wt % As, In, and Cu are also given. The results of Hashimoto[9] are

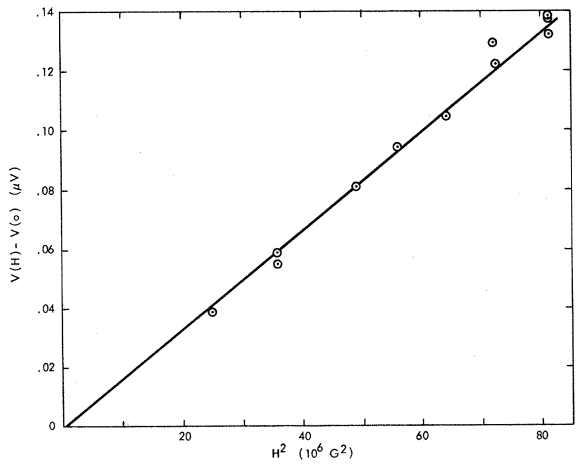

FIG. 5. Dependence of magnetovoltage on magnetic field to the second power. Bi_2Se_3 sample R12B with a current of 10 mA at 76 °K.

TABLE II. Data on single crystal Bi_2Se_3.

Sample number	Temp. (°K)	$n=\frac{1}{\rho_{213}e}$ (1/cm³) 10^{19}	ρ_{11} (Ω·m) 10^{-6}	ρ_{213} (m³/C) 10^{-7}	ρ_{321} 10^{-7}	ρ_{1111} (m⁵/C²Ω) 10^{-8}	ρ_{1122} 10^{-8}	ρ_{1133} 10^{-8}
Hashimoto (Ref. 9) 15	90	0.0215	47.6	290	275.0	27.2	44.9	498
Hashimoto 153	92	0.0321	47.3	195	209.0	11.9	42.0	73.1
Hashimoto 17	90	0.0189	10.9	331	32.1	8.44	4.51	6.8
Hashimoto 20	90	2.25	5.24	2.77	2.81	0.095	0.528	1.82
Hashimoto 173	93	2.19	3.34	2.85	2.80			0.36
R4A1	76	2.56	2.79	2.44		0.155		0.184
R6A	76	2.15	2.80	2.90		0.335		1.15
R7	76	2.94	2.36	2.12				0.202
	76	3.49	2.46	1.79		0.101		0.238
R8(1-wt%As)	76	2.15	1.48	2.90		0.182		0.265
	76	2.15	1.48	2.90		0.132		0.265
	76	2.17	1.48	2.88		0.133		0.232
R9(1-wt%In)	76	2.84	1.26	2.20		0.105		0.315
R10(1-wt%Cu)	76	0.233	12.7	26.8		0.020		2.25
R7A	76	2.40	2.70	2.60		0.106		0.148
	76	2.60	2.52	2.40				0.159
R7B	76	4.88	17.2	1.28		0.396		3.09
R12A	76	2.79	2.28	2.24	2.18	0.080	0.123	0.182
R51C	76	3.17	2.53	1.97	1.91	0.035	0.101	0.116

given for comparison. These crystals were n type with carrier concentrations in the range $2.1-3.2 \times 10^{19}$ cm^{-3}. Doping with copper reduced the carrier concentration. During the course of the experiment, several methods for attaching probes were tried. The data for crystals R4A1 through R7B (Table II) are included to demonstrate that scatter resulting from this experimentation results in too little variation to account for the difference between samples reported by Hashimoto.[9]

Data obtained on seven single crystals of Bi_2Te_3 are included in Table III. These crystals are n type ranging in concentration from 0.40 to 2.12×10^{-19} cm^{-3}. The mass ratios of the energy surfaces were calculated from the GM coefficients. The dependence of the mass ratios on carrier concentration is shown in Fig. 6 for Bi_2Te_3. All magnetoresistivity coefficients were positive except for ρ_{2323}. Although the signs of the cross-field coefficients could be determined, their magnitudes could not be measured with sufficient accuracy to warrant reporting the coefficients.

IV. DISCUSSION

In solving Eq. (2) for u, v, w, and B, we formed the following ratios of experimental data:

$$\frac{\rho_{321}}{\rho_{213}},\quad \frac{\rho_{11}\rho_{1111}}{\rho_{213}^2},\quad \frac{\rho_{11}\rho_{1122}}{\rho_{213}^2},\quad \frac{\rho_{11}\rho_{1133}}{\rho_{213}^2}$$

These ratios were taken for two reasons: (a) From an experimental point of view, these coefficients were the most accurate, and (b) from a practical point of view, they eliminated the I_n integrals which cannot be calculated unless the distribution function and the expression for the relaxation time as a function of energy are known. Other ratios have been used in the literature.[6,17]

The numerical solution of what is now a set of four equations in four unknowns was worked out

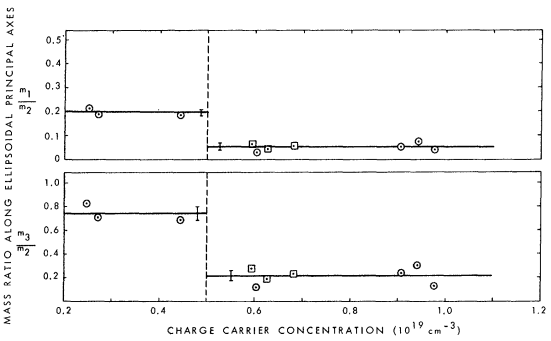

FIG. 6. Variation in the ellipsoidal energy-surface shape as a function of electron carrier concentration at 76 °K. The vertical line represents the carrier concentration above which second-band effects enter as determined from dHvA data (Ref. 5). Data points shown as squares were taken by Drabble *et al.* (Ref. 6). All low-field carrier concentrations were calculated in accordance with Eq. (5), where r was assumed equal to 1.0.

with a Newton-Raphson[29] iteration in conjunction with a Crout reduction[30] on a Univac 1108 computer. The program was used to fit the four ratios of experimental data to five figures or better whereas the actual data were "good" to no more than three figures.

Before further discussing the experimental results, something should be said regarding the accuracy of the experiments. Potential readings formed the basis for all measurements. The six-dial potentiometer was supplied with a calibration certificate indicating that on the low range the potentiometer was accurate to $\pm 0.0015\%$ of the reading $+0.1\ \mu$v. Resistivity, Hall resistivity, and current readings were large enough in magnitude to prevent this restriction from limiting the accuracy of the potential readings. The magnetoresistivity readings were voltage differences between field on and field off and, while these voltages were small in some cases (read to nearest $\pm 5\ \mu$V), the absolute error was smaller. Tests indicate a precision of $\pm 3\%$ on all GM coefficients.

The limit on the accuracy of the experimental data arises from (a) sample size measurement, (b) compositional inhomogeneities in the sample, (c) internal cracks, (d) probe misalignment, (e) orientation of the crystal, (f) localized crystal damage by the probes, and (g) field distortion within the crystal by probe contacts. Probe spacing can be determined to $\pm 1\%$ and the orientation angle to $\pm 2°$. The error from the other effects cannot be easily assessed and is larger.

The reproducibility of the data is best seen by looking at the data in Table III for samples R32A, R65A, and R63B. Each set of readings represents the average of readings for a given mounting of the potential probes and current leads. Since ρ_{11} and ρ_{1111} can be measured in either of two experimental arrangements, they also are a measure of the consistency between arrangements.

A. Bi_2Te_3

Before discussing the present results for Bi_2Te_3, we wish to comment on analyses of earlier data. Drabble *et al.*[6] were able to calculate the ratio of the effective masses of the principal axes of the valleys. Austin[12] combined the work of Drabble *et al.*[6] with his infrared Faraday rotation data and obtained the mass parameters given in Table IV. Mallinson *et al.*,[5] using the dHvA effect at 4.2 °K, have obtained shape parameters differing from those of Drabble *et al.*[6] (see Table IV). In both cases the

TABLE III. Data on single crystal Bi_2Te_3.

Sample number	$n=\frac{1}{\rho_{213}e}$ $(1/cm^3)$ 10^{+19}	ρ_{11} $(\Omega \cdot m)$ 10^{-6}	ρ_{213} (m^3/C) 10^{-7}	ρ_{321} 10^{-7}	ρ_{1111} $(m^5/C^2\Omega)$ 10^{-8}	ρ_{1122} 10^{-8}	ρ_{1133} 10^{-8}
Drabble (Ref. 9) E	1.41	1.53	4.43	9.44	7.90	11.9	27.2
Drabble C	1.24	1.68	5.05	10.13	7.75	12.7	29.0
Drabble F	1.47	1.46	4.25	8.74	7.41	11.9	25.6
R13B1	1.26	1.22	4.95		12.7		39.4
	1.28	1.19	4.86		12.3		38.4
		1.18		9.48	11.6	16.8	
R56C1		0.995		6.40	5.88	9.99	
	2.09	0.997	2.99		6.43		18.0
R56C2		1.09		5.85	6.44	10.6	
	1.84	1.12	3.40		7.17		20.5
R56B1		1.38		14.2	17.2	27.0	
	0.805	1.38	7.85		16.3		48.6
R32A		0.993		6.15	5.48	9.29	
		1.05		6.60	6.12	10.1	
	2.09	1.02	2.98		6.00		19.9
	2.12	1.02	2.94		6.14		21.1
R65A		2.56		28.0	32.4	43.9	
		2.54		28.0	32.3	41.9	
	0.400	2.56	15.6		31.9		87.9
	0.408	2.57	15.3		32.1		88.8
R63B		1.82		24.9	33.3	53.6	
		1.83		25.8	33.5	50.6	
	0.430	1.84	14.5		33.8		112
	0.428	1.86	14.6		34.0		109

TABLE IV. Shape parameters for n-type Bi_2Te_3 from GM and dHvA data.

	α_{22}	α_{11}	α_{33}	α_{23}
GM (Refs. 6 and 12)	40.0	3.9	5.4	8.9
dHvA (Ref. 5)	4.25	36.2	6.93	1.54
GM recalculated	4.12	26.8	3.72	2.4

ellipsoids are almost spheroidal; two of the axes are nearly equal and one is smaller. The magnetoresistance results indicate that the ellipsoids are compressed in a direction almost parallel to the bisectrix, while the dHvA data indicate compression parallel to the binary axis. Mallinson *et al.*[5] also have very good evidence of a higher-lying conduction minimum 30 meV above the lower-lying conduction-band minima. For large carrier concentrations, electrons begin to fill this higher band. Since the GM data were taken on crystals having charge carrier concentrations of 1.47×10^{19} cm^{-3}, while the dHvA data were taken on crystals having charge carrier concentrations of 5.3×10^{18} cm^{-3}, Mallinson *et al.*[5] surmise that the effect of the higher band on the GM data causes the discrepancy in the shape parameters of the valley. We would like to propose an additional explanation for the discrepancy in the shape parameters which will supplement the one proposed by Mallinson.

In their calculation of the mass ratios, Drabble *et al.*[6] assumed complete degeneracy because measurements of the thermoelectric power on similar samples had indicated this to be the case. This assumption enabled them to solve for B (Eq. 2) and they found it equal to unity. In the event that complete degeneracy does not hold, B will not necessarily be equal to one. We used the experimental data of Drabble *et al.*[6] (specimen F) to calculate u, v, w, and B. These results are shown in Table V. The value of B was found to be 0.705 instead of 1, indicating that the crystal was not completely degenerate. The mass parameters now indicate a relative distortion among the principal axes of the ellipsoid which is consistent with the dHvA data. One should note that Drabble[17] found that p-type Bi_2Te_3 was not completely degenerate with B equal to 0.895. Hence, there is no reason to expect complete degeneracy in n-type Bi_2Te_3 at 76 °K. The newly calculated u, v, w, and B allow the remaining resistivity ratios of the form $\rho_{11}\rho_{ijkl}/\rho_{123}^2$ to be calculated. When the value of B is known or assumed, the values of u, v, and w can be calculated exactly. As the value of B is varied from 1.0 to 0.705, the values of the mass ratios vary smoothly from the values calculated by Drabble *et al.*[6] to the recalculated ones.

Upon comparing the recalculated coefficients with those experimentally determined by Drabble *et al.*[6] (Table V), one becomes aware of a sign discrepancy in the coefficients ρ_{3211}, ρ_{1132}, and ρ_{2323}. It should be stated that all coefficients reported by Drabble *et al.*[6] were positive and it is the change in coordinate system discussed earlier that makes some of them negative in Table V. The possibility exists that the signs of the coefficients reported by Drabble *et al.*[6] were not carefully checked. Experimentally, we find the GM coefficients in n-type Bi_2Te_3 to have the signs as given by the recalculated values. Our method for calculating the GM coefficients was found consistent by recalculating the results for p-type Bi_2Te_3.[17]

We prepared samples from crystals encompassing a wide range of electron concentrations. Table VI gives the mass parameters which were calculated

TABLE V. Experimental and calculated GM coefficients for Bi_2Te_3.

	Exp (from Ref. 6)	Calc (from Ref. 6)	Recalc
ρ_{33}/ρ_{11}	...	4.1	4.15
ρ_{321}/ρ_{213}	2.06	2.06	2.06[a]
$\rho_{11}\rho_{1111}/\rho_{213}^2$	0.599	0.599[a]	0.599[a]
$\rho_{11}\rho_{1122}/\rho_{213}^2$	0.962	0.962[a]	0.962[a]
$\rho_{11}\rho_{1133}/\rho_{213}^2$	2.07[a]	2.07[a]	2.07[a]
$\rho_{11}\rho_{3211}/\rho_{213}^2$	−0.251	−0.889	0.404
$\rho_{11}\rho_{3333}/\rho_{213}^2$	...	4.53	4.787
$\rho_{11}\rho_{1132}/\rho_{213}^2$	−0.39	−0.28	0.66
$\rho_{11}\rho_{2323}/\rho_{213}^2$	0.3	−0.5[b]	−0.5
u	...	0.0979	6.506
v	...	0.134	0.904
w	...	0.0851	0.564
B	...	1.000	0.705
θ	...	±14 deg	±47 deg

[a]Fitted to experimental data. The masses were calculated from these ratios.
[b]The negative sign was omitted from Ref. 6.

TABLE VI. Mass parameters for Bi_2Te_3 and Bi_2Se_3.

Sample	$n(10^{19}$ cm$^{-3})$ $n=\frac{1}{\rho_{213}e}$	u $\frac{\alpha_{11}}{\alpha_{22}}$	v $\frac{\alpha_{33}}{\alpha_{22}}$	w $v-\left(\frac{\alpha_{23}}{\alpha_{22}}\right)^2$	B	θ deg	$\frac{m_3}{m_2}$	$\frac{m_1}{m_3}$	$\frac{m_1}{m_2}$
Bi_2Te_3 dHvA (Ref. 5)	low	7.94	1.57	1.45	···	+25.4	0.479	0.219	0.105
Bi_2Te_3 dHvA (Ref. 5)	high	8.21	1.67	1.49	···	+26.0	0.421	0.229	0.0964
Bi_2Te_3 dHS (Ref. 34)		12.9	1.49	1.44	···	+20.0	0.578	0.122	0.0707
Bi_2Te_3 Sample F (Ref. 6)	high 1.47	0.098	0.134	0.0851	1.00	+76.	0.0768	10.75	0.826
Bi_2Te_3 F Recalc. (Ref. 6)	high 1.47	6.51	0.904	0.564	0.705	+47.4	0.239	0.236	0.0565
Bi_2Te_3 E Recalc. (Ref. 6)	high 1.41	6.88	0.867	0.483	0.724	+48.1	0.199	0.226	0.0451
Bi_2Te_3 C Recalc. (Ref. 6)	high 1.24	6.22	0.862	0.596	0.720	+48.8	0.283	0.233	0.0660
Bi_2Te_3 R13B1	high 1.27	6.30	0.809	0.306	0.718	+48.8	0.116	0.257	0.0300
Bi_2Te_3 R56C2	high 1.84	5.36	0.893	0.392	0.639	+47.2	0.143	0.309	0.0441
Bi_2Te_3 R56C1	high 2.09	6.72	1.14	0.832	0.738	+41.4	0.313	0.242	0.0759
Bi_2Te_3 R32A	high 2.09	7.20	0.965	0.608	0.684	+45.8	0.244	0.220	0.0535
Bi_2Te_3 R65A	low 0.41	5.01	1.31	1.29	0.923	+19.3	0.708	0.270	0.191
Bi_2Te_3 R63B	low 0.43	4.68	1.16	1.16	0.884	+15.1	0.838	0.252	0.211
Bi_2Te_3 R56B1	low 0.80	5.05	1.32	1.30	0.856	+20.7	0.689	0.272	0.187
Bi_2Se_3 R12A	2.79	1.361	0.533	0.471	0.946	+66.5	0.383	0.814	0.312
Bi_2Se_3 R51C	3.17	1.033	0.669	0.627	0.930	+64.4	0.519	1.06	0.552

from the measured coefficients. Sample R13B1 has a carrier concentration closest to that of the samples used by Drabble *et al.*[6] and the agreement in mass parameters is fair. Included also are the parameters reported earlier by Mallinson *et al.*[5] The parameters reported by Drath and Landwehr[31] and Drath[32] were obtained from Shubnikov–deHaas (SdH) experiments using a pulsed field of up to 220 kG on iodine-doped samples. However, it is not clear whether comparison between samples doped with iodine and those doped with tellurium is valid. Ratios of the effective-mass tensor are given to show the distortion of the ellipsoids. Individual α's are obtained by combining GM data with knowledge of the density of states effective mass $m^* = (m_1m_2m_3)^{1/3}$, which can be obtained from measurements of the thermoelectric power, Faraday rotation, or some other experiment. It should also be noted that the sign of the tilt angle can be determined from Eq. (4) even when only ratios of the effective-mass tensor components are determined. It can also be obtained from dHvA experiments or SdH experiments.

One consistent trend in the data is the increase in B with decreasing carrier concentration (Table VI). When we are considering carrier densities on the order of 10^{18} cm^{-3} at 76 °K, one might expect the Fermi level to be high in the conduction band and the semiconductor therefore degenerate. The distribution is called degenerate when $kT \ll E_F$.[33] The question now is why has this not happened? Why do we determine a value for B [Eq. (2)] less than one? As a matter of fact, B deviates further from one as the carrier concentration increases. Bonch-Bruyevich[34] has made calculations for heavily doped semiconductors and has found that as a result of the interaction of charge carrier with impurity atoms, the Fermi step is "smeared out" even at $T=0$. Furthermore, the distribution function differs from the Fermi function. This might explain why the value of B becomes smaller as the carrier concentration increases and the interaction increases.

The interesting question of the concentration dependence on the shape of the constant-energy surfaces can now be looked at. Figure 6 exhibits the relevant data. While there is too much scatter in the data to determine how the mass parameters vary with concentration, there is a good indication of change in the constant energy surfaces between low- and high-concentration samples. The concentration has been calculated in accordance with Eq. (5) using $r=1$ and GF_{213} calculated from the mass ratios. The horizontal lines are root mean square values for the high and low carrier concentration ranges and the error bars are the standard deviations in these ranges. Mallinson *et al.*[5] concluded that the shape of the constant-energy surfaces for the lower band is independent of the

carrier concentration for the total carrier concentrations between 9×10^{17} and 2.4×10^{19} cm^{-3} (from high-field Hall data). This conclusion was based upon a study of the oscillation frequencies for two magnetic field directions with the sample suspended along the trigonal axis.

Mallinson *et al.*[5] found that for samples with a carrier concentration of $n=5\times10^{18}$ cm^{-3}, the carrier concentrations calculated from dHvA data were less than those calculated from Hall measurements. This was interpreted by them to mean that the higher-band electrons had a low mobility and hence did not contribute to the dHvA signal; while on the other hand, the GM results are influenced by carriers in both bands. Hence, an apparent change in energy surface shape deduced from these data might be expected. The vertical dashed line represents the concentration at which Mallinson *et al.*[5] report second-band effects entering in. The difference in mass parameters between those reported earlier and these reported recently is much greater than the difference between the high- and low-concentration samples.

The mass parameters u, v, and w from the GM and the dHvA data are now much closer than they were (Table VI). Furthermore, the data of Drabble *et al.*[6] are in reasonable agreement with the current data. The difference between the GM and dHvA data may suggest that the isotropic relaxation-time approximation does not hold. However, for some reason unclear at this time, the mass ratio may indeed change between 76 and 4 °K.

Efimova, Novikov, and Ostroumov[35] have measured the mass ratios for n-type Bi_2Te_3 at 77 °K. The results are identical to those obtained from the recalculated Drabble *et al.*[6] sample F values for m_1/m_2 and m_1/m_3 (Table VI).

The relationship between experimentally determined values and the mass parameters can best be seen in Table VII. Table VII gives the experimental data for sample R63B and the calculated values for u, v, w, and B. The effect of a ± 3% error in each of the experimental values on the mass parameter is then given. Note that, as would be expected, the mass parameters are most sensitive to error in the ρ_{321}/ρ_{213} ratio. The Hall coefficient ρ_{321} is sensitive to cracks in the sample since this voltage is measured perpendicular to the cleavage plane. From Table VII, we also see that w is very sensitive to variations in the measured coefficients; e.g., a 12% change in ω and a 25° change in θ results from a 3% change in ρ_{321}/ρ_{213}.

B. Bi_2Se_3

Measurements were made on Bi_2Se_3 samples initially to confirm the experimental arrangement and procedures by comparing with the work of Hashimoto.[9] Preliminary readings indicate that GM coefficients are much lower than he reported. Furthermore, the carrier concentration of the five identically composed samples he investigated varied from 2×10^{19} to 2×10^{17} cm^{-3}, while our data indicates no such variation. Although this variation could be accounted for by accidental doping by impurities, there has been no mention in the literature of the carrier concentration of Bi_2Se_3 being changed appreciably by doping. Indeed, a study by Miller[36] indicated that doping caused only slight changes in the carrier concentration of Bi_2Se_3.

The authors further investigated the possibility that impurities could have resulted in the data "spread" reported by Hashimoto by studying Bi_2Se_3 crystals doped with Cu, In, As, and Sn. Some results are shown in Table II. Included are the necessary GM coefficients for samples R12A and R51C from which to calculate shape parameters. Because misalignment of the probes can cause experimental errors in excess of 100% in some of the small coefficients, the cross-term magnetoresistivity coefficients are not reported. In fact, these coefficients are not needed to compute the ellipsoid mass

TABLE VII. Sensitivity of mass parameters to changes in the experimental data for sample R63B.

$\frac{\rho_{11}\rho_{1111}}{\rho_{213}^2}$	$\frac{\rho_{11}\rho_{1122}}{\rho_{213}^2}$	$\frac{\rho_{11}\rho_{1133}}{\rho_{213}^2}$	$\frac{\rho_{321}}{\rho_{213}}$	$u=\frac{\alpha_{11}}{\alpha_{22}}$	$v=\frac{\alpha_{33}}{\alpha_{22}}$	$w=v-\left(\frac{\alpha_{23}}{\alpha_{22}}\right)^2$	B	θ
(0.2900 + 0)%	(0.4496 + 0)%	(0.9493 + 0)%	(1.7223 + 0)%	(4.6778 + 0)%	(1.1647 + 0)%	(1.1624 + 0)%	(0.88386 + 0)%	15.1°
+3%				+0.51%	−0.41%	−2.3%	+0.33%	31.3°
−3%				−0.50%	+0.40%	+2.2%	−0.33%	···
	+3%			−0.48%	+3.40%	+5.2%	−0.32%	···
	−3%			+0.50%	−3.40%	−5.3%	+0.33%	34.0°
		+3%		+0.65%	−5.60%	−7.9%	−1.30%	36.8°
		−3%		−0.67%	+6.40%	+9.0%	+1.10%	···
			+3%	+3.00%	+8.30%	+14.9%	+1.93%	···
			−3%	−3.10%	−7.00%	−12.3%	−2.00%	40.3°

parameters because, once the mass parameters, u, v, w, and B have been calculated, all other magnetoresistivity coefficients can also be calculated. The work of Hashimoto[9] and Drabble *et al.*[6] showed that their measured cross-term coefficients were of the same order of magnitude as the calculated values. However, they could not be measured accurately enough to provide a good self-consistency check on the model.

The conclusion is that Hashimoto's data are basically poor for all or any of the following reasons: (a) Copper leads were used, and Cu readily diffuses in Bi_2Se_3; (b) the crystals may have contained cracks; (c) the sample geometry was not correct[37,38]; or (d) the electric field within the sample may have been distorted. The effect of copper which diffuses readily in Bi_2Se_3 is shown by the data from crystal R10. The effect of poor sample geometry is demonstrated by sample R7B, which was adjacent crystal part to R7A.

The shape parameters calculated from samples R12A and R51C are given in Table VI. One notes that the ellipsoids are not as distorted for Bi_2Se_3 as they are for Bi_2Te_3. In the case of Bi_2Se_3, the six-valley model is assumed by analogy with Bi_2Te_3. There has been no experimental or theoretical work to confirm the model.

V. CONCLUSIONS

The experimental work carried out in this study leads to several conclusions. Some of the inconsistencies that exist in the literature can be explained and a basis for further work can be laid.

The Bi_2Se_3 data show that the previously reported work of Hashimoto is in error in that samples grown with the same composition do not have widely varying carrier concentrations. This is true even when allowing for the possibility that the sample may have been accidentally doped with impurities. The carrier concentration of Bi_2Se_3 is relatively insensitive to all impurity additions tested. The appropriate shape parameters of Bi_2Se_3 are given. The error in the data of Hashimoto is believed to be due to experimental conditions of cracked samples and/or poor sample geometry.

The low-field GM coefficients of Bi_2Te_3 reported by Drabble *et al.*[6] have been used to calculate the mass parameters of the energy ellipsoids. These new mass parameters are very much more in agreement with the dHvA data of Mallinson *et al.*[5] than the earlier values reported by Drabble *et al.*[6] The reason for this is that the calculation by Drabble *et al.*[6] assumed complete degeneracy of Bi_2Te_3 while the present calculation did not. The corrected values are also in agreement with Efimova *et al.*[35]

Experimental measurements of the low-field GM coefficients for Bi_2Te_3 show considerable evidence for a change in ellipsoid shape between low-electron-concentration crystals and the high-concentration crystals which are affected by second-band effects. This is consistent with the results of Mallinson *et al.*[5] who predict that above a certain concentration, second-band effects enter. The sharp break in the mass parameters between high- and low-concentration samples could mean that high-concentration shape parameters are either a result of mixing of the two minima or that the effect of the higher-band minima is strong enough that these parameters describe only the higher band. A crystal with nearly the same concentration as was reported by Drabble *et al.*[6] compares well with their results.

The values of tilt angle as determined by GM measurements and dHvA measurements are not in good agreement with each other. Numerical results show that tilt angle is very sensitive to the GM coefficients and therefore any error is strongly reflected in the tilt angle. The remaining disagreement between dHvA mass ratios and GM mass ratios may be caused by erroneously assuming an isotropic relaxation time. To investigate this further, GM measurements must be extended to 4 °K where ionized impurity scattering should definitely predominate and hence a known value of τ may be used. There is evidence as calculated by Bonch-Bruyevich[34] that Fermi-Dirac statistics do not hold in heavily doped Bi_2Te_3.

ACKNOWLEDGMENTS

We would like to thank Dr. Roland Ure, Jr., for several helpful discussions. We are also indebted to Tony Wilcox for developing the computer programs and to Mrs. Coralyn McGregor for her assistance in preparing the manuscript.

*Work supported by the Office of Naval Research under Contract No. N-00014-67-0325-0002.

†Present address: Sandia Laboratories, Livermore, Calif. 94550.

[1]H. J. Goldsmid, J. Appl. Phys. Suppl. 32, 2198 (1961).

[2]J. R. Drabble, in *Progress in Semiconductors*, edited by A. F. Gibson and R. E. Burgess (Wiley, New York, 1963), Vol. 7, p. 45.

[3]H. J. Goldsmid, Advan. Phys. 14, 273 (1965).

[4]M. Neuberger, Hughes Aircraft Co. Electronic Properties Information Center Data Sheet No. DS-147, 1966 (unpublished).

[5]R. B. Mallinson, J. R. Rayne, and R. W. Ure, Jr., Phys. Rev. 175, 1049 (1968).

[6]J. R. Drabble, R. D. Groves, and R. Wolfe, Proc. Phys. Soc. (London) 71, 430(1958).

[7]R. W. Ure, Jr., in *Proceedings of the International*

Conference on the Physics of Semiconductors, Exeter, 1962, edited by A. C. Strickland (The Institute of Physics and the Physical Society, London, 1962), p. 659.

[8]B. Yates, J. Electron. Control 6, 26(1959).

[9]Kimio Hashimoto, J. Phys. Soc. Japan 16, 1970 (1961).

[10]G. F. Koster, in *Solid State Physics*, edited by F. Seitz and D. Turnbull (Academic, New York, 1957), Vol. 5, p. 174.

[11]J. R. Drabble and R. Wolfe, Proc. Phys. Soc. (London) 69, 1101 (1956).

[12]I. G. Austin, Proc. Phys. Soc. (London) 76, 169 (1960).

[13]F. Borghese and E. Donato, Nuova Cimento 53B, 283 (1968).

[14]D. L. Greenaway and G. Harbeke, J. Phys. Chem. Solids 26, 1585 (1965).

[15]Shin-ichi Katsuki, J. Phys. Soc. Japan 26, 58 (1969).

[16]Robert W. Keyes, J. Electron. 2, 279 (1956).

[17]J. R. Drabble, Proc. Phys. Soc. (London) 72, 380 (1958).

[18]Arthur C. Smith, James F. Janak, and Richard B. Adler, *Electronic Conduction in Solids* (McGraw-Hill, New York, 1967).

[19]D. J. Howarth, E. H. Sondheimer, Proc. Roy. Soc. (London) A219, 53 (1953).

[20]Conyers Herring, Bell System Tech. J. 34, 237 (1955).

[21]Albert C. Beer, *Solid State Physics, Suppl.* 4, *Galvanomagnetic Effects in Semiconductors*, edited by F. Seitz and D. Turnball (Academic, New York, 1963), Sec. 25.

[22]Conyers Herring and Erich Vogt, Phys. Rev. 101, 944 (1956).

[23]R. S. Allgaier, Phys. Rev. 165, 775 (1968).

[24]I. Ya. Korenblit, Fiz. Tverd. Tela 2, 3083 (1960) [Soviet Phys. Solid State 2, 2738 (1961)].

[25]B. A. Efimova, I. Ya. Korenblit, V. I. Novikov, and A. G. Ostroumov, Fiz. Tverd. Tela 3, 2746 (1961) [Soviet Phys. Solid State 3, 2004 (1962)].

[26]H. J. Mackey and J. R. Sybert, Phys. Rev. 180, 678 (1969).

[27]B. D. Cullity, *Elements of X-Ray Diffraction*, (Addison Wesley, Reading, Mass., 1956).

[28]A. Sagar and J. W. Faust, Jr., J. Appl. Phys. 38, 482 (1967).

[29]John G. Herriot, *Methods of Mathematical Analysis and Computation* (Wiley, New York, 1963), p. 73.

[30]A. M. Ostrowski, *Solution of Equations and Systems of Equations* (Academic, New York, 1966), p. 183.

[31]P. Drath and G. Landwehr, Phys. Letters 24A, 504 (1967).

[32]P. Drath, Z. Naturforsch. 23A, 1146 (1968).

[33]Charles Kittel, *Introduction to Solid State Physics* (Wiley, New York, 1956), 2nd ed.

[34]V. L. Bonch-Bruyevich, *The Electronic Theory of Heavily Doped Semiconductors* (Elsevier, New York, 1966), p. 88.

[35]B. A. Efimova, V. I. Novikov, and A. G. Ostroumov, Fiz. Tverd. Tela 4, 302 (1962) [Soviet Phys. Solid State 4, 218 (1963)].

[36]Gerald R. Miller, Masters thesis, Cornell University, 1963 (unpublished); G. R. Miller, Che-Yu Li, and C. W. Spencer, J. Appl. Phys. 34, 1398 (1963).

[37]R. F. Broom, Proc. Phys. Soc. (London) 71, 500 (1958).

[38]J. R. Drabble and R. Wolfe, J. Electron. Control 3, 259 (1957).

PHYSICAL REVIEW B VOLUME 2, NUMBER 8 15 OCTOBER 1970

Anharmonicity and the Temperature Dependence of the Forbidden (222) Reflection in Silicon†

J. B. Roberto* and B. W. Batterman

Department of Materials Science and Engineering, Cornell University, Ithaca, New York 14850

(Received 29 April 1970)

The temperature dependence of the integrated intensity of the forbidden (222) reflection in silicon has been measured from 4 to 900 °K. The results indicate that the (222) intensity at room temperature is due almost entirely to charge asymmetries introduced by the covalent bonds. However, the temperature dependence may be due to a combination of bond vibrations and anharmonicity in the atom motions. From estimates of the anharmonic contribution, and the observed temperature dependence, there is evidence that the thermal motion of the covalent bond may be different from that of the core electrons. The absolute intensity of the (222) was also measured and is consistent with $F(222) = 1.46 \pm 0.04$.

I. INTRODUCTION

In Bragg diffraction, a reflection with zero structure factor for the unit cell is termed forbidden. In the diamond structure, reflections with h, k, l mixed or h, k, l an odd multiple of 2 should be forbidden from a lattice point consideration. Nevertheless, in 1921 Bragg[1] found a weak x-ray reflection at the forbidden (222) position in diamond.

Silicon crystallizes in the diamond structure, and a similar anomalous reflection appears at the (222). Since spherical atoms at the lattice sites yield a zero structure factor, this forbidden intensity must be due to some perturbation on the spherical atoms. Further, since the x rays interact only with the electron charge distribution of an atom,